Available online at www.sciencedirect.com
SCIENCE DIRECT®
Journal of Organometallic Chemistry 679 (2003) 84–92
Journal of Organometallic Chemistry
www.elsevier.com/locate/jorganchem

# Density functional study of lanthanide complexes $(\eta^5\text{-}C_5H_5)_2LnX\cdot OC_4H_8$ (Ln = La–Lu; X = F, Cl, Br and I)

Yi Luo [a], Parasuraman Selvam [a,1], Yuki Ito [a], Akira Endou [a], Momoji Kubo [a], Akira Miyamoto [a,b,*]

[a] Department of Materials Chemistry, Graduate School of Engineering, Tohoku University, Aoba-yama 07, Sendai 980-8579, Japan
[b] New Industry Creation Hatchery Center (NICHe), Tohoku University, Aoba-yama 04, Sendai980 8579, Japan

Received 24 February 2003; received in revised form 4 June 2003; accepted 5 June 2003

**Abstract**

Density functional calculations were performed on a series of mixed-ligand organolanthanide complexes, $(\eta^5\text{-}C_5H_5)_2LnX\cdot OC_4H_8$ ($\eta^5\text{-}C_5H_5$ = Cp; Ln = La–Lu; X = F, Cl, Br and I; $OC_4H_8$ = THF). The calculated geometrical parameters are in reasonable agreement with the experimental data. The distances between Ln and ligands follow linearity along the ionic radius of lanthanide metal, as the same as that observed in experiment. In the mixed-ligand complexes, Ln–Cp and Ln–THF bonds are more covalent compared to Ln–X. The lanthanide contraction of various bond and the metal–ligand interaction energy followed the order of Ln–X > Ln–Cp > Ln–$OC_4H_8$. The orbital population and dipole moment were also discussed.


*Keywords:* Organolanthanide; Density functional theory; Molecular structure; Lanthanide contraction and charge population; Orbital composition

## 1. Introduction

Electronic structure of molecular systems containing f elements has been the object of numerous experimental [1] and theoretical [2] studies. In this framework, one of the more challenging topics is the 'chemical' description of the lanthanide–ligand or actinide–ligand interactions in terms of ionic versus covalent interaction [3]. This point is of great importance for a better understanding of the molecular properties of lanthanide and actinide series, such as stability or reactivity. For instance, improvement of chemical processes involved in the nuclear waste treatment may be expected from a better basic description of these interactions [4]. Theoretical investigations are therefore useful to get more insight into the lanthanide– or actinide–ligand interactions within various kinds of molecular environments. Unfortunately, a precise evaluation of molecular properties is still far from being a routine task, especially when f electrons are involved. In fact, a reliable theoretical tool must be able to yield, at the same time, precise geometrical and thermodynamic results and a detailed chemical analysis of the electronic structure. Such a tool requires a sufficiently accurate treatment of the two main physical effects that dominate the chemistry and physics of heavy metals, i.e., relativity and electron correlation. Different relativistic contributions play a significant role in heavy metal chemistry [5] and can be described by different approaches [6], ranging from four component fully relativistic Dirac–Fock methods [7] to two-component approximations resulting from the Foldy–Wouthuysen [8] or the Doulas–Kroll transformations of the Dirac Hamiltonian [9] to the very cheap and popular relativistic effective core potential approaches (RECP) [10]. A number of studies [11] show that DFT methods based on the generalized gradient approximations (GGA) can model with remarkable accuracy the properties of heavy elements. Even better results can be obtained by the so-called self-consistent hybrid approaches [12]. Furthermore, these methods are particularly powerful for a chemist, since their mono-determinantal nature allows an easy-to-read interpreta-

* Corresponding author. Tel.: +81-22-217-7233; fax: +81-22-217-7235.
*E-mail address:* miyamoto@aki.che.tohoku.ac.jp (A. Miyamoto).
[1] On sabbatical leave from the Department of Chemistry, Indian Institute of Technology-Bombay, Powai, Mumbai 400 076, India.

0022-328X/03/$ - see front matter © 2003 Elsevier B.V. All rights reserved.
doi:10.1016/S0022-328X(03)00517-5

tion of the results. The implementation of relativistic models in the DFT has been achieved at different precision levels, such as the zero-order regular approximation [13]. Furthermore, it has been shown that standard RECP's provide accurate description also in DFT schemes [14]. The above mentioned studies document the DFT methods are able to capture the main features of metal–ligand interactions, at least for complexes involving first- and second-row transition metals. The situation is more crucial for lanthanide and actinide complexes, since the reliability of DFT methods in describing on the same footing correlation and relativistic effects has also been carried out on small model system, such as lanthanide chalcogenide and hydrides [2b,11b]. Hence, it will be interesting to investigate whether GGA approaches provide a sufficiently reliable description of the bonding in organolanthanide complexes.

The model $(\eta^5\text{-}C_5H_5)_2LnX\cdot OC_4H_8$ ($\eta^5\text{-}C_5H_5 = Cp$, $OC_4H_8 = THF$, Ln = La–Lu, X = F, Cl, Br and I) complexes were found to be good candidates for our purpose, as they have been the subject of numerous experimental studies [15]. Moreover, the use of halogen ligands leads to a modulation of the chemical environment of the lanthanide from a hard anion ($F^-$) to a soft, polarizable anion ($I^-$), providing a useful framework for further analysis of the electronic structure in terms of various chemical environments.

The chemistry of the trivalent lanthanide ions has expanded rapidly in the latter part of the last century. The interest in the lanthanide complexes is chiefly ruled by their promising utilization due to their low toxicity and their powerful paramagnetic and luminescent properties [16] as well as their use in biological systems [17]. Organolanthanide chemistry has witnessed a dramatic progress in the past two decades and currently receiving a significant attention, especially in C–H bond activation studies. Among these, lanthanide metallocene complexes are the most extensively studied organolanthanide compounds, on which many general and comprehensive reviews have already appeared [18]. In this development, alkyl and hydrido complexes bearing two substituted or unsubstituted cyclopentadienyl ligands have occupied an especially important place because of their high activity and unique behavior in various catalytic processes [19]. The investigation of the physico-chemical properties and reactivity of lanthanide compounds attracts many interests, due to their importance in various fields, such as photoluminescence or biological and medical applications and chemical process involved in the nuclear industry catalytic reaction as well as organic synthesis [20].

Organolanthanoid chemistry is dominated by complexes of charged π donor ligands, such as cyclopentadienide ($C_5H_5^-$), pentamethylcyclopentadienide ($C_5Me_5^-$), and cyclooctatetraenide ($C_8H_8^-$). And mixed-ligand complexes with charged π donors, neutral donors, such as tetrahydrofuran (THF), and/or anionic ligand, e.g. halide or aryloxide, were well established [15b,21]. As often happens, the experimental interest has determined a parallel growth of theoretical work, mainly devoted to the understanding of the nature of rare earth–ligand interactions. It is important for the development of organolanthaniods in the synthesis and application to understand the binding behavior of Ln and ligand at electron level. Although the theoretical calculation studies on the lanthanide complexes appear to be complicated due to the large effects of relativity and electron correlation, some successful density functional calculations have been performed on lanthanide complexes with charged or uncharged π donor and anionic or neutral donors, respectively [22]. Otherwise, based on our knowledge, mixed-ligand trivalent lanthanide complex, which contains charged π donor, anionic and neutral donors in one molecule, was not noticed in theoretical field until now. One of the reasons may be the expensive calculation cost because of larger molecular system. Lanthanide contraction is one important character for lanthanide compounds and was discussed in many theoretical studies [2b]. However, the theoretical estimation of lanthanide contraction for various coordinate bonds in one molecule containing mixed-ligand is still lacking. The present study focus on the mixed-ligand organolanthanide complexes, $Cp_2LnH$ (Ln = La–Lu, X = F, Cl, Br and I). Since there exists some difficulties in the synthesis of lanthanide complex, especially for the difficulties in crystallization, it is difficult to get the structure data for these lanthanide complexes. Our calculation result is expected to give some hints to the determination of the geometry structure for these lanthanide complexes in the present study. The lanthanide contractions of different coordination bond, charge and several orbital populations have been discussed also.

## 2. Computational details

The present density functional theory (DFT) calculations were performed by using the Amsterdam density functional package (ADF 2000.02) [23], at the level of GGA. The choice of PW91XC functional [24] was made for GGA exchange and correlation correction. The relativistic corrections of the atomic cores are taken into account. The quasi-relativistic approach of Pauli Hamiltonian often fails to give acceptable results for very heavy elements even a frozen core basis set [13]. Taking this into account, the zero-order regular approximation (ZORA) formalism [13,25] was applied, and the ZORA basis sets were provided by ADF package. The 4f orbital was included in the valence shell of lanthanides atoms. The $ns^2np^5$ ($n = 2$, 3, 4 and 5), $2s^22p^2$ and

$2s^2 2p^4$ electrons were taken as valence electrons for halides, carbon and oxygen, respectively. Triple-zeta Slater type orbital basis functions were used for all the elements, and two polarization functions given in ADF package were added for main group elements, viz. 2p and 3d for H; 3d and 4f for C, O and Cl. Because of unpaired electrons of Ln atoms, spin-unrestricted calculations were performed for all of the complexes used in this study without symmetry constraint.

## 3. Results and discussion

### 3.1. Bond lengths, bond angles and lanthanide contractions

As shown in Fig. 1, the two ring centroids plus the halide and oxygen atom of THF describe a distorted tetrahedral geometry of $Cp_2LnX(THF)$. The similarity of the structures can be best seen by examining the compilation of values of distances and angles given in Tables 1 and 2. The available X-ray diffusion data (XRD) [15a–c] were listed in the parenthesis. Comparing the experimental distance with the corresponding calculated ones, one finds that they are very well agreement with each other. The Yb–Cp distances of 2.388–2.415 Å for the various complexes (cf. Table 1) are in good agreement with that of 2.402 Å reported for $Cp_2Yb{\cdot}DME$ [15d]. In a similar way, lanthanocene complexes such as bis(tetrahydrofurfurylindenyl) lanthanocene chloride, show 2.678–2.545 Å for Ln–Cl, and 2.509–2.391 Å for Ln–Cp (Ln = Nd, Sm, Gd, Dy, Ho, Er, Yb) [15e]. The corresponding data listed in Table 1 are consistent with these experimental findings. With regard to the angles in Table 2, The calculated ones in $Cp_2YbI(THF)$ and $Cp_2LuCl(THF)$ can be better compared to the experimental ones with the deviation of $<4^\circ$. In the case of $Cp_2SmCl(THF)$ and $Cp_2SmI(THF)$, the angles O–Ln–X are consistent with the available XRD data. However, the calculated angles Cp–Sm–Cp are lower than the experimental ones by nearly $10^\circ$, which may result from the replacement of hydrogen with methyl in the π-ligand.

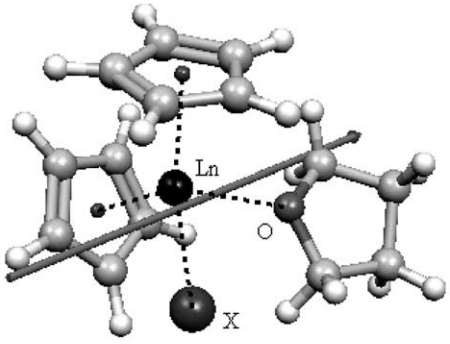


Fig. 1. The geometry structure of $Cp_2LnX(THF)$. (Cp = cyclopentadienyl, THF = tetrahydrofuran, Ln = La–Lu and X = halides. Unmarked white and gray balls represent hydrogen and carbon, respectively. The arrow indicates the direction of dipole moment.)

Comparing the La–F distance in $Cp_2LaF(THF)$ with the La–I distance in $Cp_2LaI(THF)$, one finds that the difference is 0.96 Å. Followed the same strategy, the differences between Ln–F and Ln–I distances in other complexes were found to be in the scope of 0.92–0.96 Å. These differences can be compared to a 0.9 Å difference normally assumed between the sizes of fluoride and iodide ions [26]. In contrast to the large variation observed in metal–halides distance when halide size is accounted for, the distances of the metal to the centroid of Cp ring (Ln–Cp) do not vary substantially from those expected. In the comparison of $Cp_2LnF(THF)$ and $Cp_2LnI(THF)$, the distance Ln–Cp in $Cp_2LnI(THF)$ are shorter only by 0.02–0.04 Å, which shows the very slight approaches of metal toward Cp ring with the increase of the halide in size. This case can be understood by that the larger halide prefers to slightly pushing metal into Cp ligands.

It is well known that the filling of 4f shell causes lanthanide contraction [2b] ($\Delta R_{\text{lanthanide}}$), which can be defined as: $\Delta R_{\text{lanthanide}} = R(\text{LaL}) - R(\text{LuL})$, where $R$(LaL) and $R$(LuL) represent the bond lengths of lathanum–ligands and lutetium–ligands, respectively. Based on the distance listed in Table 1, $\Delta R_{\text{lanthanide}}$ was investigated for Ln–X, Ln–O and Ln–Cp bonds in $Cp_2LnX(THF)$ complex, which were presented in Table 3. The values for the lanthanide contractions are found to depend strongly on the ligand [27]. In $Cp_2LnX(THF)$ complex, the values of lanthanide contraction are found to vary from 0.015 to 0.217 Å. From Table 3, it is easy to be aware of that the values of both Ln–Cp and Ln–O bond contractions decrease slightly from F to I complex, which indicated that the strength of Ln–Cp and Ln–O bonds increase from F to I [27]. This also illustrates that the presence of halides ligands (F, Cl, Br and I) brings certain effect on the lanthanide contraction of the Ln–Cp and Ln–O bonds in the mixed-ligand complex. In the case of Ln–X bond contraction, the value of Ln–I bond contraction seems to be out of the increase tendency from F to Br. The same result was observed in other lanthanide compounds [28]. For organolanthanide compounds, it is announced experimentally [29] that the metal–ligands distances follow a linear trend along with the increasing metal ionic radius. The similar trends were also observed based on our theoretical results for $Cp_2LnX(THF)$, which were illustrated in Fig. 2. For a comparison, the data of several binary compounds, viz. $MCl_3$ and $Cp_3M$ (M = La, Ce, Eu, Gd, Yb and Lu), are also included in this figure. As expected, both these compounds show a high correlation coefficient ($R^2$). On the other hand, the functions Y(Ln–O) and Y(Ln–Cp) are not so smooth (lower $R^2$) compared to the Y(Ln–X) functions (X = F, Cl, Br

Table 1
The selected bond lengths (Å) in $Cp_2LnX(THF)$; Ln = La–Lu, X = F–I

| Complex | Bond [a] | X = F | X = Cl | X = Br | X = I |
|---|---|---|---|---|---|
| $Cp_2LaX(THF)$ | La–X | 2.176 | 2.708 | 2.889 | 3.14 |
| | La–O | 2.460 | 2.463 | 2.464 | 2.463 |
| | La–Cp | 2.519 | 2.49 | 2.485 | 2.475 |
| $Cp_2CeX(THF)$ | Ce–X | 2.146 | 2.672 | 2.853 | 3.105 |
| | Ce–O | 2.463 | 2.464 | 2.466 | 2.465 |
| | Ce–Cp | 2.466 | 2.446 | 2.444 | 2.441 |
| $Cp_2PrX(THF)$ | Pr–X | 2.128 | 2.655 | 2.835 | 3.088 |
| | Pr–O | 2.457 | 2.454 | 2.456 | 2.456 |
| | Pr–Cp | 2.457 | 2.437 | 2.436 | 2.429 |
| $Cp_2NdX(THF)$ | Nd–X | 2.115 | 2.639 | 2.818 | 3.071 |
| | Nd–O | 2.450 | 2.440 | 2.443 | 2.444 |
| | Nd–Cp | 2.459 | 2.433 | 2.432 | 2.426 |
| $Cp_2PmX(THF)$ | Pm–X | 2.109 | 2.631 | 2.811 | 3.068 |
| | Pm–O | 2.452 | 2.448 | 2.449 | 2.447 |
| | Pm–Cp | 2.455 | 2.443 | 2.437 | 2.428 |
| $Cp_2SmX(THF)$ | Sm–X | 2.114 | 2.627(2.71) | 2.806 | 3.063(3.04) |
| | Sm–O | 2.447 | 2.449(2.44) | 2.452 | 2.450(2.45) |
| | Sm–Cp | 2.453 | 2.441(2.45) | 2.440 | 2.430(2.44) |
| $Cp_2EuX(THF)$ | Eu–X | 2.116 | 2.622 | 2.803 | 3.062 |
| | Eu–O | 2.430 | 2.436 | 2.439 | 2.441 |
| | Eu–Cp | 2.465 | 2.447 | 2.445 | 2.433 |
| $Cp_2GdX(THF)$ | Gd–X | 2.081 | 2.580 | 2.759 | 3.013 |
| | Gd–O | 2.428 | 2.437 | 2.440 | 2.443 |
| | Gd–Cp | 2.418 | 2.402 | 2.401 | 2.397 |
| $Cp_2TbX(THF)$ | Tb–X | 2.066 | 2.564 | 2.743 | 2.998 |
| | Tb–O | 2.428 | 2.439 | 2.443 | 2.444 |
| | Tb–Cp | 2.405 | 2.394 | 2.391 | 2.384 |
| $Cp_2DyX(THF)$ | Dy–X | 2.051 | 2.550 | 2.730 | 2.987 |
| | Dy–O | 2.423 | 2.434 | 2.438 | 2.439 |
| | Dy–Cp | 2.404 | 2.392 | 2.392 | 2.384 |
| $Cp_2HoX(THF)$ | Ho–X | 2.044 | 2.544 | 2.723 | 2.982 |
| | Ho–O | 2.425 | 2.432 | 2.436 | 2.437 |
| | Ho–Cp | 2.407 | 2.390 | 2.389 | 2.381 |
| $Cp_2ErX(THF)$ | Er–X | 2.040 | 2.543 | 2.721 | 2.983 |
| | Er–O | 2.430 | 2.423 | 2.427 | 2.427 |
| | Er–Cp | 2.407 | 2.395 | 2.394 | 2.385 |
| $Cp_2TmX(THF)$ | Tm–X | 2.043 | 2.534 | 2.713 | 2.977 |
| | Tm–O | 2.416 | 2.426 | 2.430 | 2.429 |
| | Tm–Cp | 2.409 | 2.400 | 2.397 | 2.388 |
| $Cp_2YbX(THF)$ | Yb–X | 2.041 | 2.529 | 2.710 | 2.957(2.93) |
| | Yb–O | 2.402 | 2.416 | 2.421 | 2.427(2.31) |
| | Yb–Cp | 2.415 | 2.402 | 2.398 | 2.388(2.30) |
| $Cp_2LuX(THF)$ | Lu–X | 2.007 | 2.493(2.50) | 2.672 | 2.936 |
| | Lu–O | 2.422 | 2.445(2.27) | 2.447 | 2.448 |
| | Lu–Cp | 2.373 | 2.361(2.29) | 2.360 | 2.352 |

The data in parenthesis were taken from X-ray diffraction results [15a–c].
[a] The Ln–Cp means the average distance between the Ln ion and the centroids of Cp rings.

and I), which reflects the stronger covalence of Ln–O and Ln–Cp bonds compared to Ln–X bond [30].

### 3.2. Charge population

The theoretical limitations of Mulliken charge population are well known, especially for the interaction between metal and ligand [31]. Otherwise, the limitation of Mulliken charge need be further investigated for lanthanide complex by systematic theory calculation. Without going into details, the descriptions of Mulliken charge were published elsewhere [32]. Figs. 3 and 4 plotted the variety of Mulliken charge bared by lanthanide and halides atoms through the whole lanthanide series. The charge population on halides (Fig. 4) shows the ion character of X–Ln bond decreases as the order: F > Br > Cl > I. The same consequence can be also seen from Fig. 3. It is clear that the charge on Br is more negative than that on Cl, which contradicts the usual chemical idea that the electronegativity of Cl is greater than that of Br. On the other hand, the charge on Ln atom in all of the four kinds of complex decreases

Table 2
The selected angles (°) in $Cp_2LnX(THF)$; Ln = La–Lu, X = F–I

| Complex | Angle [a] | X = F | X = Cl | X = Br | X = I |
|---|---|---|---|---|---|
| $Cp_2LaX(THF)$ | Cp–Ln–Cp | 115.3 | 117.4 | 117.8 | 118.6 |
| | O–Ln–X | 87.8 | 92.7 | 94.1 | 95.5 |
| $Cp_2CeX(THF)$ | Cp–Ln–Cp | 119.3 | 120.9 | 121.1 | 121.3 |
| | O–Ln–X | 85.1 | 90.7 | 92.3 | 94.5 |
| $Cp_2PrX(THF)$ | Cp–Ln–Cp | 120.1 | 121.7 | 121.8 | 122.4 |
| | O–Ln–X | 86.6 | 91.0 | 92.4 | 94.0 |
| $Cp_2NdX(THF)$ | Cp–Ln–Cp | 119.1 | 122.0 | 122.1 | 122.7 |
| | O–Ln–X | 85.7 | 91.3 | 92.4 | 94.2 |
| $Cp_2PmX(THF)$ | Cp–Ln–Cp | 120.2 | 121.2 | 121.7 | 122.5 |
| | O–Ln–X | 83.0 | 91.3 | 92.7 | 94.1 |
| $Cp_2SmX(THF)$ | Cp–Ln–Cp | 120.3 | 121.4(133) | 121.5 | 122.5(136) |
| | O–Ln–X | 86.7 | 91.0(90.4) | 92.5 | 94.0(90.5) |
| $Cp_2EuX(THF)$ | Cp–Ln–Cp | 119.4 | 120.9 | 121.0 | 122.0 |
| | O–Ln–X | 85.7 | 91.2 | 92.7 | 94.2 |
| $Cp_2GdX(THF)$ | Cp–Ln–Cp | 123.4 | 124.8 | 124.9 | 121.1 |
| | O–Ln–X | 85.5 | 90.1 | 91.2 | 92.7 |
| $Cp_2TbX(THF)$ | Cp–Ln–Cp | 124.5 | 125.6 | 125.8 | 126.5 |
| | O–Ln–X | 85.5 | 89.5 | 90.9 | 92.2 |
| $Cp_2DyX(THF)$ | Cp–Ln–Cp | 124.5 | 125.7 | 125.7 | 126.4 |
| | O–Ln–X | 85.6 | 89.3 | 90.8 | 92.1 |
| $Cp_2HoX(THF)$ | Cp–Ln–Cp | 124.4 | 125.9 | 126 | 126.7 |
| | O–Ln–X | 84.7 | 90.0 | 91.0 | 92.2 |
| $Cp_2ErX(THF)$ | Cp–Ln–Cp | 124.3 | 125.4 | 125.5 | 126.4 |
| | O–Ln–X | 83.2 | 89.4 | 90.8 | 92.2 |
| $Cp_2TmX(THF)$ | Cp–Ln–Cp | 124.1 | 125.0 | 125.2 | 126.1 |
| | O–Ln–X | 85.1 | 89.3 | 90.7 | 91.9 |
| $Cp_2YbX(THF)$ | Cp–Ln–Cp | 123.6 | 124.8 | 125.1 | 126.1(129.8) |
| | O–Ln–X | 85.1 | 89.6 | 90.9 | 92.1(92.0) |
| $Cp_2LuX(THF)$ | Cp–Ln–Cp | 127.5 | 128.7(129) | 128.8 | 129.6 |
| | O–Ln–X | 85.0 | 88.2(91.6) | 89.1 | 90.1 |

The available experimental data [15a–c] are listed in parenthesis.
[a] The Cp–Ln–Cp means the angle of two Cp ring centroids and Ln ion.

slightly in going from La to Lu complex (Fig. 3). This trend can be also found in other lanthanide compounds [33]. Furthermore, the charge born by halides is almost constant throughout the whole lanthanide series (Fig. 4). This illustrates that the Mulliken charge population on halides ligands was almost not affected by lanthanide metal.

### 3.3. Ligand–metal interaction energies

We estimated the metal–ligand binding energies for the $Cp_2LnX(THF)$ as shown in Fig. 5. For the sake of simplicity, we only selected La, Gd and Lu complexes, in which the metals located in the initial, middle and the end of lanthanide series, respectively. The interaction energy of per kind of ligand was defined by $2\Delta E(\text{Ln–Cp}) = E\ [Cp_2LnX(THF)] - E\ [LnX(THF)] - E\ (Cp_2)$, $\Delta E(\text{Ln–X}) = E\ [Cp_2LnX(THF)] - E\ [Cp_2Ln(THF)] - E\ (X)$ and $\Delta E(\text{Ln–THF}) = E\ [Cp_2LnX(THF)] - E\ (Cp_2LnX) - E\ (THF)$, respectively, where E represents the bond energies of the corresponding species. The more negative $\Delta E$ value implies the stronger binding strength of ligand toward metal. It is need to mention here the basis set superposition error (BSSE) was found to be lower than 1.5% of interaction energy for trivalent lanthanide complexes of terpyridine and was omitted in the calculation of the interaction energy of lanthanide metal with terpyridine ligand [34]. Moreover, it is declared that there was only variation of 0.1–0.7 eV in $Ln–C_6H_6$ bond dissociation energy when spin-orbital coupling was accounted [35]. On the other hand, in this work, we are interested in the interaction energy of various ligands with a given metal, which is quite different. Hence, the BSSE and spin-orbital coupling is considerably out of consideration in the present analysis. Fig. 5 shows that ligand binding strength follows the

Table 3
The lanthanide contraction ($\Delta R_{\text{lanthanide}}$; Å) of several bonds in $Cp_2LnX(THF)$; Ln = La and Lu

| Bond | X = F | X = Cl | X = Br | X = I |
|---|---|---|---|---|
| Ln–X | 0.169 | 0.215 | 0.217 | 0.204 |
| Ln–O | 0.038 | 0.018 | 0.017 | 0.015 |
| Ln–Cp | 0.146 | 0.129 | 0.125 | 0.123 |

$\Delta R_{\text{lanthanide}} = R(\text{LaL}) - R(\text{LuL})$; L = X, O or Cp.

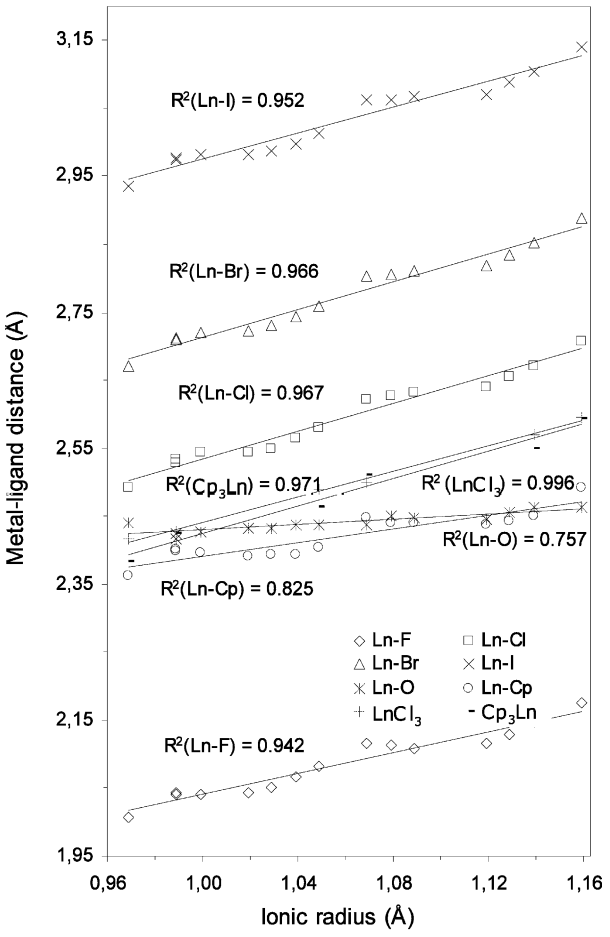


Fig. 2. The relationship between the metal-ligands distances (Ln–X, Ln–O and Ln–Cp) and metal ionic radius in $Cp_2LnX(THF)$ complex.

sequence of X > Cp > THF. However, in the case of $Cp_2LnI(THF)$ complex, the binding energies toward metal of Cp and I ligands are close. In the mixed-ligand complex selected in his study, the neutral ligand, THF,

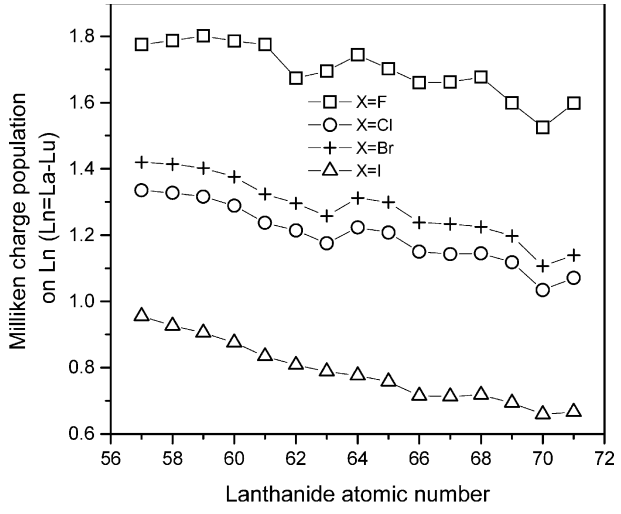


Fig. 3. The Mulliken charge population on Ln in $Cp_2LnX(TFH)$ complexes (Ln = La–Lu, X = halides).

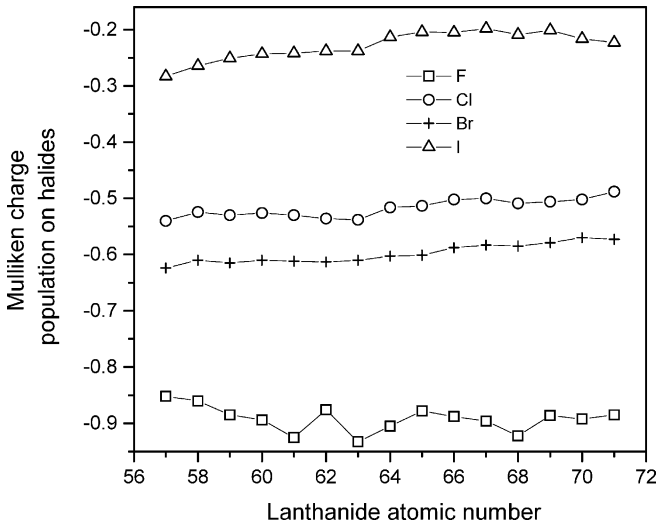


Fig. 4. Mulliken charge population on halides in $Cp_2LnX(TFH)$ complex (Ln = La–Lu, X = halides).

shows weaker binding energy compared to charged Cp and X ligands. These diversities resulted from various binding nature of ligands. The binding strength of halides with metal decreases in the sequence of F > Cl > Br > I (Fig. 5), and the same trend was observed in lanthanide trihalides [36]. This can be explained based on the increase in the atomic radius, which in turn results in the lower electron density between the lanthanides and halides.

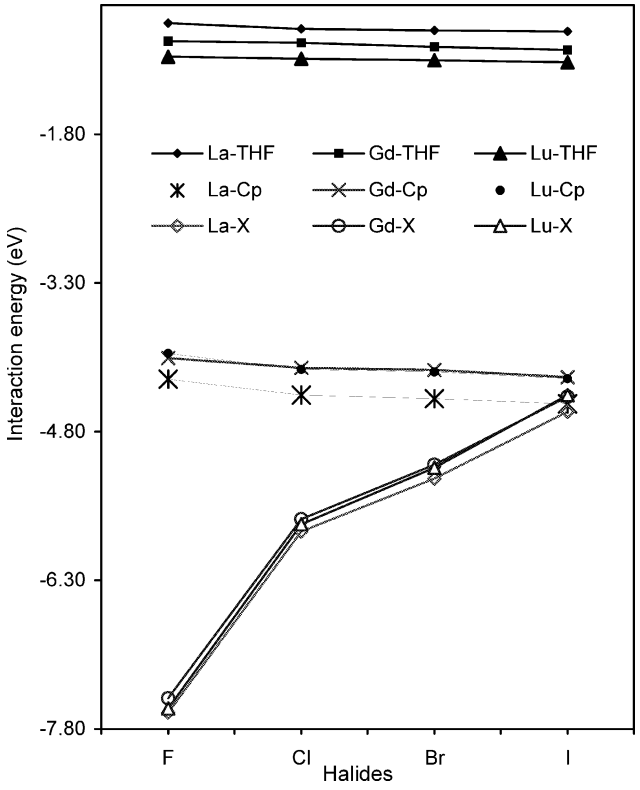


Fig. 5. Metal–ligand binding energy in the complexes.

### 3.4. Atomic and molecular orbital

In order to investigate the effects of halides and lanthanide metal on atomic and molecular orbital of $Cp_2LnX(THF)$ complex, following the same strategy as in the above binding energy analysis, we have selected three kinds of metal complexes, $Cp_2LaX(THF)$, $Cp_2GdX(THF)$ and $Cp_2LuX(THF)$. The Mulliken valence electron population of metal atomic orbital (AO) and the composition of highest occupied molecular orbital (HOMO) and lowest unoccupied molecular orbital (LUMO) in the selected complexes were presented in Table 4. In the case of halides, the bond orbitals are mainly due to $n$p ($n = 2$, 3, 4 and 5) atomic orbital. Hence, the population on the atomic orbital of halides was not listed in Table 4. In this calculation, $1s^2 2s^2 2p^6 3s^2 3p^6 3d^{10} 4s^2 4p^6 4d^{10}$ was taken as effective core potentials of Ln. Hence, in Table 4, the valence electron population on s orbital means the total population on 5s and 6s and the p-orbital population includes that of Ln-5p and Ln-6p atomic orbital. The populations on d and f-orbital mean that on Ln-5d and Ln-4f orbital, respectively. As shown in Table 4, the population on s orbital is slightly over 2, which suggests that 6s-orbital acts as main electron donor in the complexes. From Table 4, it is clear that all of the Ln-5d populations are more than 1 in the complexes, which indicates that Ln-5d orbital act as electron acceptor in the interaction of Ln with ligands. This observation also can be obtained from our recent calculation [11b]. Moreover, the population on Ln-5d increases slightly in the sequence of F < Br < Cl < I, which corresponding to the sequence of Mulliken charge population. The valence electron population on La-5p is almost around 6, which illustrated that La-5p nearly does not take part in the formation of chemical bond. Otherwise, in the case of Gd and Lu complex, especially for their chloride, bromine and iodine complexes, the Gd-6p and Lu-6p orbitals contributed clearly to bonding because of the over 6 population on p orbital (Table 4). The populations on 4f orbital were increased slightly compared with that of free Ln atoms. There is an exception for Lu complexes because of full-filled 4f shell. Table 4 also indicates that the HOMO mainly consists of the AO in Cp and X-$n$p (X = halides; $n = 3$, 4 and 5) orbital. It is need to mention here that the contribution lower than 5% is not considered for this analysis. In each kind of metal complex, the contribution of the AO in Cp to HOMO decreases in the sequence of F > Cl > Br > I, however, the contribution of X-$n$p orbital increases in accordance with the order of F < Cl < Br < I. However, the compositions of LUMO depend clearly upon the metal ions (Table 4). The empty La-4f and partially filled Ln-4f as well as Ln-5d orbitals contribute to LUMO. In the case of La and Lu complexes, the AOs in Cp also contribute to LUMO. However, in the case of Gd complex, LUMO mainly consists of half-filled Gd-4f orbital.

### 3.5. Dipole moment

DFT method was widely used to determine the molecular properties, such as geometry structure and dipole moments, in the framework of quantum chemistry. The magnitudes of dipole moments for the selected complex molecules were plotted against lanthanide atomic number (Fig. 6). All of the magnitudes of the dipole moments were calculated at the optimized

Table 4
The population of AO and the composition of HOMO and LUMO in the selected complexes $Cp_2LnX(THF)$ (Ln = La, Gd and Lu, X = F, Cl, Br and I)

| Complex | Metal atomic valence shell | | | | The composition of molecular orbital (%) | |
|---|---|---|---|---|---|---|
| | s | p | d | f | HOMO | LUMO |
| $Cp_2LaX(THF)$ | | | | | | |
| F | 2.03 | 5.85 | 1.00 | 0.35 | 96Cp | 33La5d+16La4f+43Cp |
| Cl | 2.08 | 5.98 | 1.28 | 0.34 | 81Cp | 30La5d+30La4f+27Cp |
| Br | 2.08 | 5.96 | 1.22 | 0.33 | 78Cp+6Br4p | 31La5d+32La4f+26Cp |
| I | 2.12 | 6.08 | 1.53 | 0.32 | 45Cp+41I5p | 35La5d+29La4f+26Cp |
| $Cp_2GdX(THF)$ | | | | | | |
| F | 2.06 | 5.97 | 1.05 | 7.17 | 83Cp | 98Gd4f |
| Cl | 2.14 | 6.14 | 1.33 | 7.17 | 67Cp+12Cl3p | 96Gd4f |
| Br | 2.15 | 6.12 | 1.25 | 7.16 | 66Cp+22Br4p | 96Gd4f |
| I | 2.19 | 6.27 | 1.60 | 7.17 | 38Cp+53I5p | 96Gd4f |
| $Cp_2LuX(THF)$ | | | | | | |
| F | 2.03 | 6.18 | 1.16 | 14.02 | 83Cp | 35Lu5d+14Lu6s+23Cp |
| Cl | 2.16 | 6.37 | 1.38 | 14.02 | 74Cp+15Cl3p | 47Lu5d+7Lu6s+26Cp |
| Br | 2.17 | 6.34 | 1.34 | 14.02 | 74Cp+15Cl3p | 47Lu5d+7Lu6s+26Cp |
| I | 2.25 | 6.50 | 1.57 | 14.02 | 34Cp+56I5p | 57Lu5d+5Lu6s+24Cp |

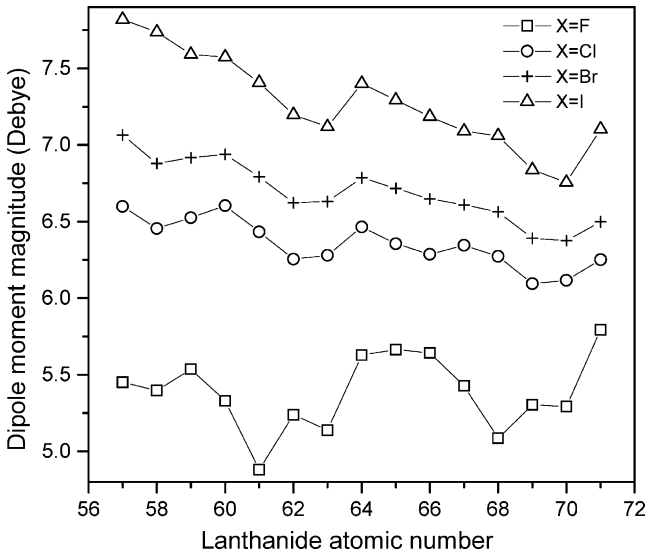


Fig. 6. Dipole moment magnitudes of the complexes molecules.

structure. Although the calculation of dipole polarizability was found to depend on the basis set and functional [35], the results of dipole moment calculated by the same functional are worth of relative investigation when the same basis set is employed. Moreover, larger basis set with sufficient diffuse basis sets is benefit to produce more accurate results [37], and Triple-zeta polarized was used in our calculation. Hence, it is expected to get more reasonable result compared to smaller basis set, such as double-zeta basis set. In spite of the data error resulted from method, the various tendency of dipole moment discussed here is expected to be reliable because of the application of the same method. As an example, the direction of dipole moment of $Cp_2GdBr(THF)$ molecule was shown in Fig. 1 (see the arrow direction). It is clear that the vector didn't take the axial direction of Gd–Br bond. The dipole moment vectors of residual complex molecules were almost along the same direction as that of $Cp_2GdBr(THF)$. Fig. 6 indicates that the dipole moments of complex molecules decrease slightly upon lanthanide serials except for fluorine complexes. The exception for fluorine complex may be imputed to that stronger interaction of F with central Ln ions counteracted the slight decrease trend along lanthanide serials. On the other hand, the dipole moment magnitudes of complex molecules decreased in the order of $I > Br > Cl > F$ (Fig. 6). It is not strange because the polarization of Ln–X bond counteracted the dipole moment of complex molecules.

## 4. Conclusion

The mixed-ligand complex $(\eta^5\text{-}C_5H_5)_2LnX\cdot OC_4H_8$ (Ln = La–Lu; X = halide) was investigated by DFT calculation. The lanthanide contraction varies with different coordination bond, which decreases in the sequence of Ln–X > Ln–Cp > Ln–O. Moreover, the lanthanide contraction of the same bond type, saying Ln–Cp or Ln–O, was influenced by surrounding halides. The linear relationships were observed between Ln–ligand bond lengths and metal ionic radius, and the lower correlation coefficients of Ln–Cp and Ln–O linear equations showed their more covalent characters compared to Ln–X bond. In the mixed-ligand complex, the binding energy of neutral ligand THF toward metal is smaller than that of charged ligand, e.g. Cp and halides. In the case of halides, the interaction energy toward the same metal was decreased by the increase of halides atom radius. The orbital analysis based on the present DFT calculation showed that Ln-6s orbital acts as main electron donor and Ln-5d is one acceptor. The HOMO of the complex mainly consists of the atomic orbital of Cp and the $n$p ($n = 2$, 3, 4 and 5) orbital of halides, however, the compositions of LUMO contain the atomic orbital of Ln and the Cp ligand.

## References

[1] (a) F.T. Edelmann, D.M.M. Freckmann, H. Schumann, Chem. Rev. 102 (2002) 1851;
(b) W.J. Evans, B.L. Davis, Chem. Rev. 102 (2002) 2119.
[2] (a) C.P. Groen, A. Oskam, A. Kovacs, Inorg. Chem. 39 (2000) 6001;
(b) M. Dolg, H. Stoll, in: K.A. Gschneidner, Jr, L. Eyring (Eds.), Handbook on the Physics and Chemistry of Rare Earths, Ch. 152, vol. 22, Elsevier, New York, 1996.
[3] (a) D.L. Clark, J.C. Gordon, P.J. Hay, R.L. Martin, R. Poli, Organometallics 21 (2002) 5000;
(b) D.M. Guldi, T.D. Mody, N.N. Gerasimchuk, D. Magda, J.L. Sessler, J. Am. Chem. Soc. 122 (2000) 8289.
[4] (a) L. Joubert, P.J. Maldivi, Phys. Chem. 105 (2001) 9068;
(b) F. Arnaud-Neu, J.K. Browne, D. Byrne, D.J. Marrs, M.A. McKervey, P. O'Hagan, M.J. Schwing-Weill, A. Walker, Chem.-A Eur. J. 5 (1999) 175.
[5] (a) P. Belanzoni, E. van Lenthe, E.J. Baerends, J. Chem. Phys. 114 (2001) 4421;
(b) G. Schreckenbach, T. Ziegler, Int. J. Quantum Chem. 61 (1997) 899.
[6] (a) K.G. Dyall, J. Comput. Chem. 23 (2002) 786;
(b) W. Kutzelnigg, J. Comput. Chem. 20 (1999) 1199.
[7] (a) S. Varga, A. Rosen, W.D. Sepp, B. Fricke, Phys. Rev. A. 6302 (2001) 2510;
(b) Y. Watanabe, O. Matsuoka, J. Chem. Phys. 116 (2002) 9585.
[8] M. Barysz, A.J. Sadlej, J. Chem. Phys. 116 (2002) 2696.
[9] M. Barysz, Acta Phys. Pol. A. 101 (2002) 815.
[10] A. Bergner, M. Dolg, W. Kueche, H. Stoll, H. Preuss, Mol. Phys. 80 (1993) 1431.
[11] (a) P. Lantto, J. Vaara, A.M. Kantola, V.V. Telkki, B. Schimmelpfennig, K. Ruud, J. Jokisaari, J. Am. Chem. Soc. 124 (2002) 2762;
(b) Y. Luo, X. Wan, Y. Ito, S. Takami, M. Kubo, A. Miyamoto, Chem. Phys. 282 (2002) 197;
(c) X. Wan, X. Wang, Y. Luo, S. Takami, M. Kubo, A. Miyamoto, Organometallics 21 (2002) 3703.

[12] M. Thoss, H.B. Wang, W.H. Miller, J. Chem. Phys. 115 (2001) 2991.
[13] E. van Lenthe, A. Ehlers, E.J. Baerends, J. Chem. Phys. 110 (1999) 8943.
[14] (a) W.A. de Jong, R.J. Harrison, J.A. Nichols, D.A. Dixon, Theor. Chem. Acc. 107 (2001) 22;
(b) Y. Luo, X. Wan, Y. Ito, S. Takami, M. Kubo, A. Miyamoto, Appl. Surf. Sci. 202 (2002) 283.
[15] (a) W.J. Evans, J.W. Grate, K.R. Levan, I. Bloom, T.T. Peterson, R.J. Doedens, H. Zhang, J.L. Atwood, Inorg. Chem. 25 (1986) 3614;
(b) G.B. Deacon, S.C. Harris, G. Meyer, D. Stellfeldt, D.L. Wilkinson, G. Zelesny, J. Organomet. Chem. 525 (1996) 247;
(c) Z. Ni, Z.M. Zhang, D.L. Deng, C.T. Qian, J. Organomet. Chem. 306 (1986) 209;
(d) J. Jin, S. Jin, W. Chen, J. Organomet. Chem. 412 (1991) 71;
(e) J. Cheng, D. Cui, W. Chen, T. Tang, B. Huang, J. Organomet. Chem. 658 (2002) 153.
[16] (a) M. Sakamoto, K. Manseki, H. Okawa, Coord. Chem. Rev. 219 (2001) 379;
(b) V. Vicinelli, P. Ceroni, M. Maestri, V. Balzani, M. Gorka, F. Vogtle, J. Am. Chem. Soc. 124 (2002) 6461.
[17] E. Pidcock, G.R. Moore, J. Biol. Inorg. Chem. 6 (2001) 479.
[18] (a) G.A. Molander, J.A.C. Romero, Chem. Rev. 102 (2002) 2161;
(b) K.C. Hultzsch, T.P. Spaniol, J. Okuda, Organometallics 16 (1997) 4845.
[19] (a) Y.W. Li, T.J. Marks, J. Am. Chem. Soc. 120 (1998) 1757;
(b) A.A. Trifonov, T.P. Spaniol, J. Okuda, Organometallics 20 (2001) 4869.
[20] Y. Li, T.J. Marks, Organometallics 15 (1996) 3770.
[21] C.Z. Ni, Z.M. Zhang, D.L. Deng, C.T. Qian, J. Organomet. Chem. 306 (1986) 209.
[22] (a) L. Maron, O. Eisenstein, J. Phys. Chem. A 104 (2000) 7140;
(b) C. Rabbe, V. Mikhalko, J.P. Dognon, Theor. Chem. Acc. 104 (2000) 280.
[23] G. te Velde, F.M. Bickelhaupt, E.J. Baerends, C. Fonseca Guerra, S.J.A. van Gisbergen, J.G. Snijders, T. Ziegler, J. Comput. Chem. 22 (2001) 931.
[24] J.P. Perdew, Y. Wang, Phys. Rev. B 46 (1992) 6671.
[25] E. van Lenthe, J.G. Snijders, E.J. Baerends, J. Chem. Phys. 105 (1996) 6505.
[26] D.R. Lide, Handbook of Chemistry and Physics, Section 12, 79th ed., CRC, Washington, DC, 1998–199.
[27] W. Kuchle, M. Dolg, H. Stoll, J. Phys. Chem. A 101 (1997) 7128.
[28] C. Adamo, P. Maldivi, Chem. Phys. Lett. 268 (1997) 61.
[29] J. Oliver, Jr, W.S. Rees, Inorg. Chem. 40 (2001) 1751.
[30] N.R. Kenneth, Jr, C.W. Eigenbrot, Acc. Chem. Res. 13 (1980) 276.
[31] (a) R.S. Mulliken, J. Chem. Phys. 23 (1995) 1833;
(b) F. De Profit, J.M.L. Martin, P. Geerling, Chem. Phys. Lett. 50 (1996) 393.
[32] (a) R.S. Mulliken, J. Chem. Phys. 23 (1995) 1833;
(b) R. Dronskowski, P.E. Bloechl, J. Phys. Chem. 97 (1993) 8617.
[33] (a) C. Boehme, B. Coupez, G. Wipff, J. Phys. Chem. A 106 (2002) 6487;
(b) F. Berny, N. Muzet, L. Troxler, A. Dedieu, G. Wipff, Inorg. Chem. 38 (1999) 1244.
[34] C. Rabbe, V. Mikhalko, J.P. Dognon, Theor. Chem. Acc. 104 (2000) 280.
[35] H. Lu, L. Li, Theor. Chem. Acc. 102 (1999) 121.
[36] C. Adamo, P. Maldivi, J. Phys. Chem. A 102 (1998) 6812.
[37] O.N. Ventura, M. Kieninger, I. Cernusak, J. Mol. Struct. 436–437 (1997) 489.